Reactive extrusion of biodegradable PGA/PBAT blends to enhance flexibility and gas barrier properties

Christopher Ellingford[a#], Paresh Kumar Samantaray[a#], Stefano Farris[b], Tony McNally [a], Bowen Tan[c], Zhaoyang Sun[c], Weijie Huang[c], Yang Ji[c], Chaoying Wan[a]*

[a] International Institute for Nanocomposites Manufacturing (IINM), WMG, University of Warwick, CV4 7AL, U.K.

[b] Department of Food, Environmental and Nutritional Sciences, University of Milan, 20133, Milano, Italy

[c] PJIM Polymer Scientific Co., Ltd., Shanghai, 201102, China

*Corresponding author: Chaoying.Wan@warwick.ac.uk

#equal contribution

ABSTRACT

Among commercial biodegradable polyesters, poly(glycolic acid) (PGA) has been rarely investigated for packaging applications, despite its unique advantages such as 100% compostability, high degree of crystallinity, high thermal stability and high gas barrier properties. The application of PGA has been limited by its mechanical brittleness, moisture sensitivity, and high melting temperature (~240 ^{o}C), restricting its processing and applications for film packaging. In this study, PGA was modified by blending with poly (butylene adipate-co-terephthalate) (PBAT) via melt-extrusion. A commercial terpolymer of ethylene, acrylic ester and glycidyl methacrylate (EMA-GMA) was selected for compatibilization. The phase morphology, rheology, thermal, mechanical and gas barrier properties of the blends were investigated. With addition of 20 wt. % EMA-GMA, the elongation of PGA/PBAT (50/50 wt. %) blends was improved from 10.7 to 145%, the oxygen permeability was reduced from 125 to 103 (cm^3 mm) / (m^2 24h atm), and the water vapour barrier performance was improved by ~47%. The enhancement in ductility, oxygen and water vapor barrier properties of the flexible blends were ascribed to the interfacial bonding between PBAT and PGA enabled by EMA-GMA. The compatibilized PGA/PBAT blends with high thermal stability up to 300 ^{o}C are preferable for high temperature or hot food packaging.

INTRODUCTION

Bioplastics refer to polymers that are derived from the biomass, such as bio-polyethylene and bio-poly(ethylene terephthalate) but are not biodegradable or those derived from either biomass (e.g. poly (lactic acid), PLA) or petrochemicals (e.g. PGA) and are biodegradable.[1] It implies that bioplastics have two aspects of sustainability, green educt and/or green product. While green educt implies the bioplastics generated from the feedstock or derived biologically, green product implies that the derivative products will be degradable and have a low impact on the environment.[2] Further, life-cycle analyses of bioplastics indicate that they can reduce carbon dioxide (CO_2) emissions by 30~70% compared with conventional plastics.[3] Interestingly, in a recent market data report by the Nova Institute, bioplastics are shown to represent ~ 1 % of the annual plastics production at 359 million tonnes.[3] With intriguing sophisticated applications and emerging biodegradable alternatives, the market for bioplastics is increasing rapidly. Whilst the current global production capacity is estimated to be around 2.11 million tonnes, it is expected to increase and diversify production up to 2.43 million tonnes by 2024.[3]

PLA is the most commonly used biodegradable bioplastic in the market.[4] Despite its good mechanical strength and melt-processability, it's brittleness, low gas barrier properties, and slow rate of degradation limit its applications for food packaging. In this regard, its chemical analogue, poly (glycolic acid) PGA, exhibits higher mechanical strength, higher heat distortion temperature, and exceptional gas barrier properties due to its higher degree of crystallinity (~50 %). In addition, PGA has a faster degradation rate than PLA and is also 100% compostable under both industrial and domestic composting conditions.[4-5] Although PGA is known to have high production cost, PJCHEM China has circumvent this bottleneck by synthesizing economically viable PGA from syngas that utilizes carbon monoxide from coal waste gases which would have otherwise be burnt to CO_2 and contributed to greenhouse effect.[4] The only key challenge in PGA's direct application to film packaging is the high degree of crystallinity of PGA that leads to mechanical brittleness.

Poly(butylene adipate-co-terephthalate) (PBAT) is an aliphatic-aromatic biodegradable polyester that has an exceptional extension at break.[6-7] It is often blended with other polymers such as PLA for enhancing ductility and toughness,[8-11] where a good compatibility between the polymer components is a prerequisite.[6] PGA being a structural analogue of PLA has a similar solubility parameter (δ_{PGA}: 23.5 $MPa^{1/2}$) as PLA (δ_{PLA}: 20.2 $MPa^{1/2}$), also faces similar compatibility challenges when blended with PBAT. Reactive extrusion has been successfully applied in melt-processing of polymer blends with *in-situ* compatibilization. Using a free radical initiator dicumyl peroxide (DCP), *in-situ* compatibilization was realised during melt-blending of PLA and PBAT.[12] Inclusion of 0.5 wt. % DCP, PLA/PBAT (80/20 wt. %) blends showed greater compatibility through reduced PBAT domain size, yielding a strain at break of up to 300%, combined with increased toughness and tensile strength.

Due to the uncontrolled nature of this approach, products including branched and crosslinked PLA or PBAT, PLA-g-PBAT copolymers and PLA crosslinked with PBAT could not be avoided.

The chain end groups, carboxylic acid, in PLA and PBAT are often used for reactive extrusion with chain extenders for compatibilization.[13] For example, 2,2'-(1,3-phenylene)bis(2-oxazoline) and phthalic acid were used in tandem in a PLA/PBAT (80/20, wt. %) blend demonstrated high strain (516%) and high strength (45.3 MPa). The increased interfacial adhesion between PLA and PBAT, as well as a decrease in the crystallinity of the blend was attributed to the enhanced mechanical performance. Furthermore, trans-esterification of PLA/PBAT *via* 0.4 wt. % tetrabutyl titanate led to a PLA/PBAT (70/30, wt. %) blend demonstrating high strength and elongation through enhanced interface compatibility.[14]

PLA and PBAT blends were also compatibilized using cellulose nanocrystals (CNCs). CNCs had stronger thermodynamical affinity towards the PBAT phase, while with higher CNC loadings (3 wt. % and 5 wt. %), the CNCs were found mainly at the interface and in the PLA phase. This led to an appreciable Young's modulus for the composite but low extension at break of 4 % for 5 wt. % CNC loading.[15] In other work, Cardolite®NC-514, a bio-based epoxy-cardanol pre-polymer (ECP) was used for compatibilizing PLA/PBAT blends. It was observed that the ECP content of less than 3 wt. % could effectively compatibilize the blend and showed significant improvement in elongation at break and a slight increment in tensile strength compared to the non-compatibilized blends. The ECP showed better interfacial compatibilization for PLA/PBAT blends than for Joncryl ADR 4300 (a multi- functional epoxy chain extender by BASF) for the same concentration.[16] Abdelwahab et al. used glycidyl methacrylate monomer as a toughening agent for PLA and organosolv lignin based polymer blends. It was observed that by blending glycidyl methacrylate with PLA, the elongation at break was enhanced from 3.3% to 401%.[17] This result suggests that epoxy-based compatibilizers may also work for compatibilizing PGA and PBAT blends.

In this work, we investigate the compatibilization of EMA-GMA, a commercial terpolymer of ethylene, methyl acrylate, and glycidyl methacrylate for PGA/PBAT (50/50, wt. %) blends prepared by melt-extrusion. The phase morphology, rheology, thermal and mechanical properties were studied, the moisture and oxygen barrier performance evaluated at 23°C and 65 % RH and, 23°C, 0 % and 50 % RH, respectively. The results revealed that these blends were effectively compatibilized and can be suitably used in flexible packaging films.

MATERIAL AND METHODS

Materials

PGA was supplied by PJIM Polymer Scientific Co. Ltd. with an average number molecular weight of 10^5 g/mol. PBAT (Ecoflex Blend F C1200) supplied by BASF has an average number

molecular weight of 1.42×10^5 g·mol^{-1}. A terpolymer of ethylene, methyl acrylate, and glycidyl methacrylate (EMA-GMA) with 8 wt. % glycidyl methacrylate and 24 wt. % methyl acrylate with the trade name LOTADER®AX8900 was kindly gifted by SK Functional Polymers. Its average number molecular weight is 4.5×10^4 g·mol^{-1}.

Blend preparation

Prior to extrusion, PGA and PBAT were dried in a desiccant dryer overnight at 65 °C. PGA/PBAT (50/50 wt. %) was blended with AX8900 at loadings between 10-30 wt. % via melt-extrusion using an Eurolab 16 (Thermo Fisher Scientific) twin-screw extruder with an L/D ratio of 40:1. The extrusion temperature zones were set from 220 °C to 240 °C, the feed was set at 6 %, and a screw speed of 120 rpm was used for all experiments.

Blend characterization

Fourier-Transform Infrared spectroscopy (FTIR) was performed on a Bruker TENSOR 27 instrument in the spectral range 4000 to 650 cm^{-1} at a resolution of 4 cm^{-1} with 64 scans. Differential scanning calorimetry (DSC) was carried out using a Mettler Toledo DSC 1. 5-8 mg of a polymer was placed within a DSC pan and then analyzed under a constant nitrogen flow rate of 50 mL/min. The experiments were performed using 10 K/min for both heating and cooling cycles. For mechanical testing, blends were pelletized and injection moulded as per ASTM D 638 standards using a Haake Minijet Pro piston injection moulding machine. The mechanical testing was performed on a 250 kN Static Instron with a 10 kN fixture and a strain rate of 10 mm/min up to 110 % elongation and then at 25 mm/min until the sample broke. Scanning electron microscopy (SEM) was performed using a Carl Zeiss Sigma Field SEM using an InLens detector under a 5 kV operating voltage. Prior to imaging, samples were cryo-fractured and sputter coated using a Au/Pd target. Oscillatory rheology measurements were carried out using a HAAKE MarsIII Rheometer at 240 °C in the frequency range 0.008 – 100 Hz. Oxygen transmission rate (OTR) and water vapour transmission rate (WVTR) were measured using a Totalperm permeabilimeter by Permtech, according to ASTM 3985 (OTR at 23°C and 0% RH), ASTM F1927 (OTR at 23 °C and 50% RH) and ASTM F1249 (WVTR at 23°C and 65% RH). To reset any influence arising from different film thicknesses, transmission rate values were converted to permeability coefficients – $P'O_2$ (cm^3·mm·m^{-2} 24h atm) and P′WV (g·mm·m^{-2} 24h atm). Scheme 1(a) shows the flow chart of the overall experimental process of this work.

RESULTS AND DISCUSSION

For the formation of polymer blends, the miscibility and resulting phase morphology is key for achieving optimal mechanical and gas barrier properties. To visualise the effect of introducing EMA-GMA, the cryo-fractured surfaces of the blends was imaged using SEM, see Figure 1. Prior to the addition of EMA-GMA, 50/50 PGA/PBAT exhibits large phase separation, with spherical PBAT

domains with over 100 µm in diameter residing in a PGA continuous phase. With 10 wt. % addition of EMA-GMA as shown in Figure 1 b), phase separation still exists but the dispersed phase is more homogeneous, indicating that 10 wt. % of EMA-GMA is not sufficient to bridge the PGA and PBAT phases at a 50/50 weight ratio. Upon addition of 20 wt. % EMA-GMA, no sharp interfaces is observed between PGA and PBAT phases. This indicates that at 20 wt. % EMA-GMA, the PGA and PBAT phases are compatibilized. However, subtle evidences of phases merged together can still be observed in 50/50/20 indicated by grey spherical regions highlighted in red in figure 1c) With 30 wt. % EMA-GMA, a homogenous phase is observed (Figure 1d)), indicating the interfacial interactions and compatibilization between PGA and PBAT is enhanced by inclusion of EMA-GMA. The absence of sharp interfaces between PGA and PBAT helps in effective stress transfer between phases during mechanical properties.

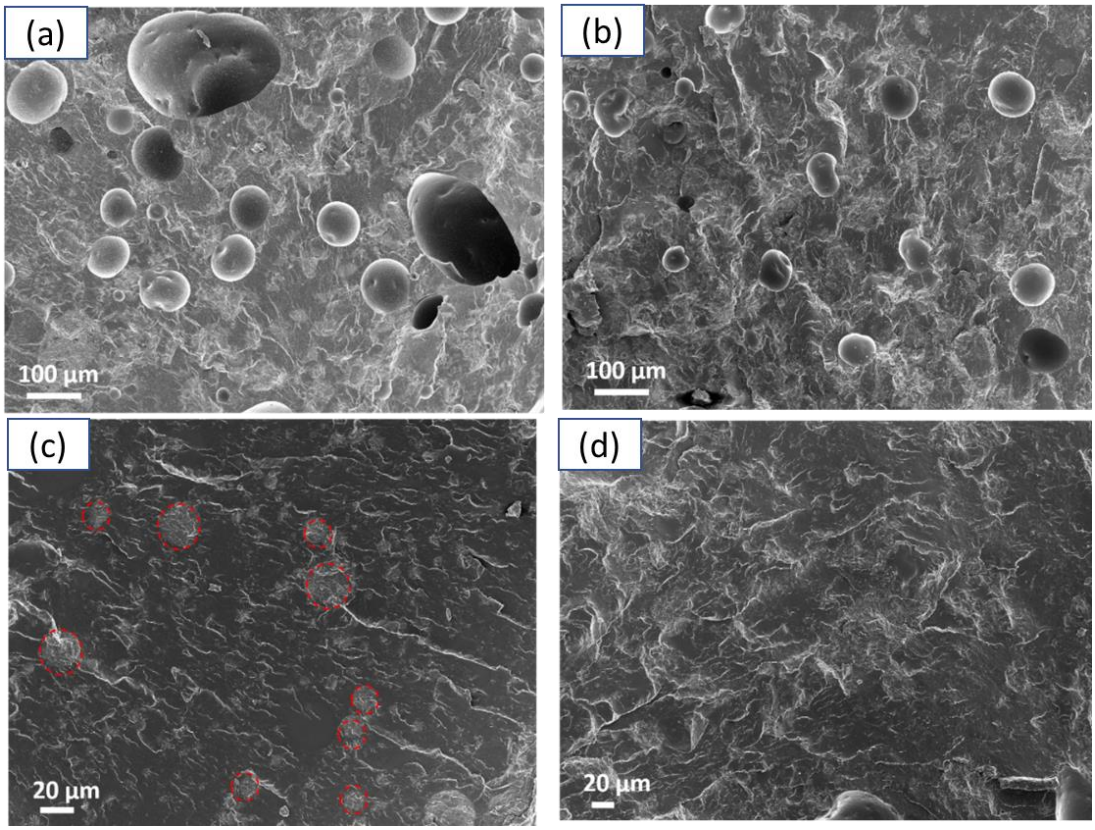

Figure 1: SEM images of cryo-fractured surface of a) PGA/PBAT (50/50), b) PGA/PBAT/EMA-GMA (50/50/10), c) PGA/PBAT/ EMA-GMA (50/50/20) and d) PGA/PBAT/ EMA-GMA (50/50/30) blends.

The nature of the compatibilization between PGA, PBAT and EMA-GMA was investigated *via* FTIR, see Figure 2. Pristine PGA shows an ester C=O stretching band at 1737 cm^{-1}, whilst pristine PBAT shows the -C=O stretching band at 1711 cm^{-1}. Furthermore, a broad OH stretching band is observed in PBAT at approximately 3400 cm^{-1}. In PGA/PBAT 50/50, the PGA ester stretching peak shifts to 1733 cm^{-1} while the PBAT ester stretch shifts to 1720 cm^{-1}, attributed to a change in the chemical surroundings for each polymer, affecting their site-specific interactions.[18] Specifically, this

includes weak hydrogen bonding between C-H and O groups in CH_2 and ether groups in PGA, respectively[19] and a conjugative effect between phenylene aromatic and carbonyl groups in PBAT[18, 20-21]. The -OH stretching due to PBAT was also observed at approximately 3500 cm^{-1}. With the addition of 10 wt. % EMA-GMA, the shift in ester and carbonyl groups is prominent at 1731 cm^{-1} and 1715 cm^{-1} but a change in PGA ester intensity was observed with respect to PBAT, indicating that some of the PGA ester groups were hydrogen bonding with the hydroxyl group of EMA-GMA.

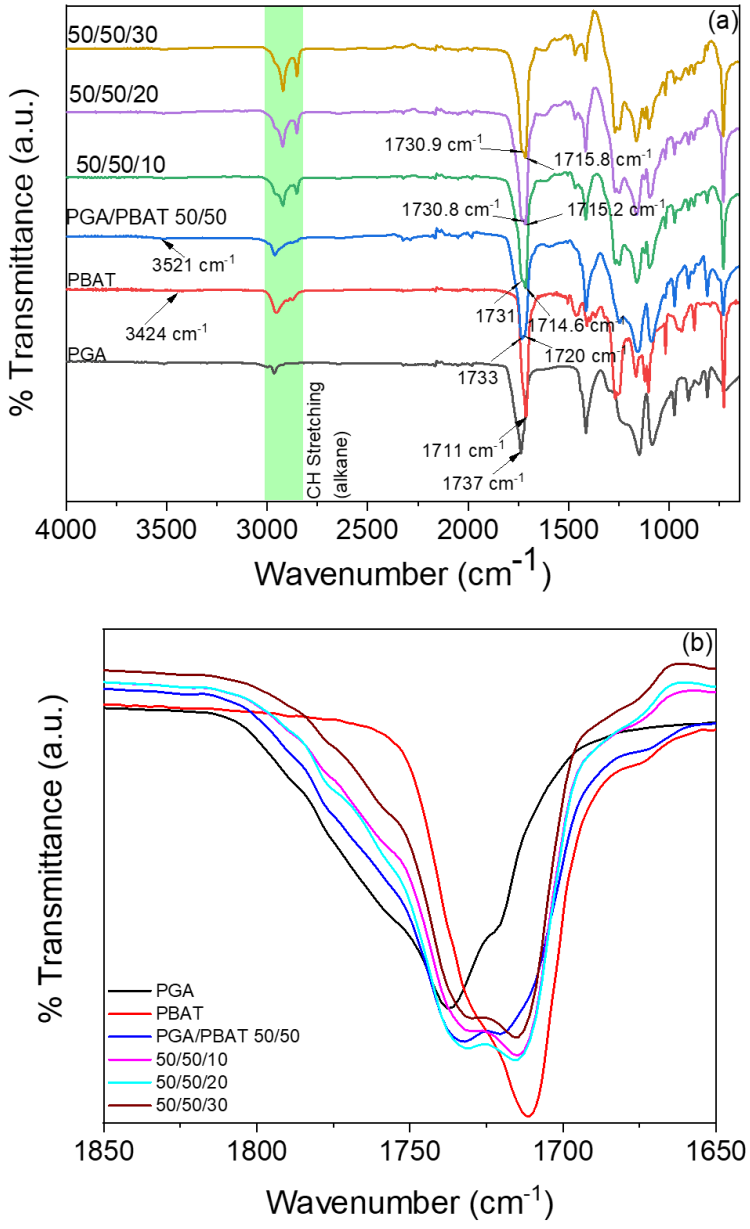

Figure 2: (a) FTIR spectra of the polymers and blends of PGA, PBAT, PGA/PBAT (50/50) with between 10 and 30 wt. % EMA-GMA and (b) FTIR spectra showing the change in the ester peak for the same set of materials.

In addition, the -OH stretching observed in the PGA/PBAT/EMA-GMA (50/50/10) blend broadened and shifted to a lower wavenumber, indicating further that the newly formed hydroxyl group of EMA-GMA interacted with esters along the PBAT and PGA chains. Similar observations were also seen in the blends containing 20 wt. % and 30 wt. % EMA-GMA, where the shift in the PGA ester and PBAT ester are observed at 1731 and 1715 cm^{-1}, respectively for the 20 wt. % EMA-GMA blend and 1731 and 1716 cm^{-1}, respectively, for the 30 wt. % EMA-GMA blend. The free carboxylic acid end group of PBAT can react with the glycidyl end of EMA-GMA to form ester derivatives as per the mechanism proposed by Shechter et al,[22] as well as hydrogen bond with PBAT through the ester groups. In comparison EMA-GMA has been shown to only have a partial miscibility when the PGA structural analogue, PLA, is used, indicating that its compatibilization of PGA/PBAT may be somewhat limited.[23] Therefore, sufficient glycidyl groups are required for this compatibilization reaction, and since EMA-GMA only contains 8 wt. % of glycidyl moieties, we therefore selected a concentration > 10 wt. % in this study.

Therefore, based on the FTIR result, the following compatibilization mechanism is presented in Scheme 1(b). We propose that the EMA-GMA acts as a compatibilizer through the ring opening of the epoxide group *via* the carboxylic acid chain end, which then allows PGA esters to interact with the newly formed hydroxyl group from partially miscible EMA-GMA/PBAT.

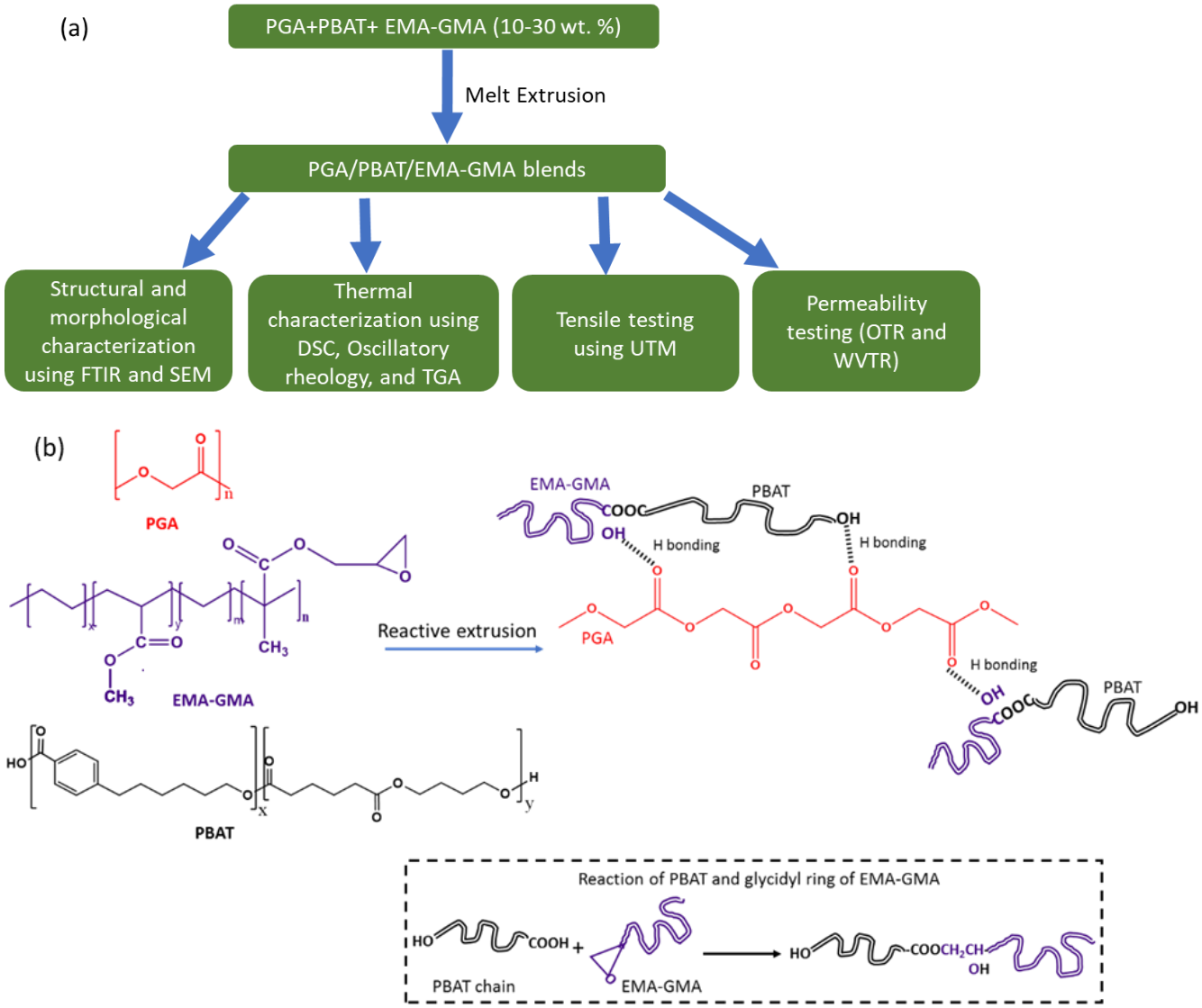

Scheme 1: (a) Flowchart of the synthesis and characterization process in this work. (b)Schematic representation of the compatibilization interaction between PGA, PBAT, and EMA-GMA during extrusion.

The development of phase morphology of the PGA/PBAT blend induced by inclusion of EMA-GMA can be reflected by the change in the viscoelastic behaviour of the polymer blends, see Figure 3. When 10 wt. % compatibilizer is introduced, the storage modulus (G′), loss modulus (G″) and complex viscosity (|η*|) of the polymer blend are unaffected across the entire frequency range examined. However, a deviation in the linear relationship between G′ and G″ in the Cole-Cole plot, Figure 3 c), indicates that the polymer blends demonstrate an increased elastic response after compatibilization. This is due to interactions between >10 wt. % EMA-GMA with PGA and PBAT, confirming the interactions detected by FTIR. After introducing 20 wt. % EMA-GMA, both the G′ and G″, and complex viscosity of PGA/PBAT (50/50) increased by one order of magnitude. In addition, the Cole-Cole plot shows further, strong deviation in the linear relationship between the elastic modulus (G′) and G″. Overall, this

confirms that EMA-GMA is compatibilizing PGA and PBAT and significantly altering its physical properties. Finally, after the addition of 30 wt. % EMA-GMA, a further increase of one order of magnitude is observed in the G′ and |η*|, but not the G″, demonstrating an increase in the elastic behaviour of the blend. The greater deviation in the linear relationship in the Cole-Cole plot shows that 30 wt. % EMA-GMA further increases the compatibility between PGA/PBAT, which is reflected in the mechanical properties shown in Figure 4. Furthermore, as the compatibilizer content is increased in PGA/PBAT (50/50), the crossover point for the liquid-to-solid like behaviour transition of the polymer blend occurs at higher frequencies, at 0.05 Hz, 0.9 Hz and 27 Hz for 10, 20 and 30 wt. % EMA-GMA additions, respectively. Without EMA-GMA, this transition is not observed, see Figure 3 e), demonstrating the increased elastic behaviour of the blend.

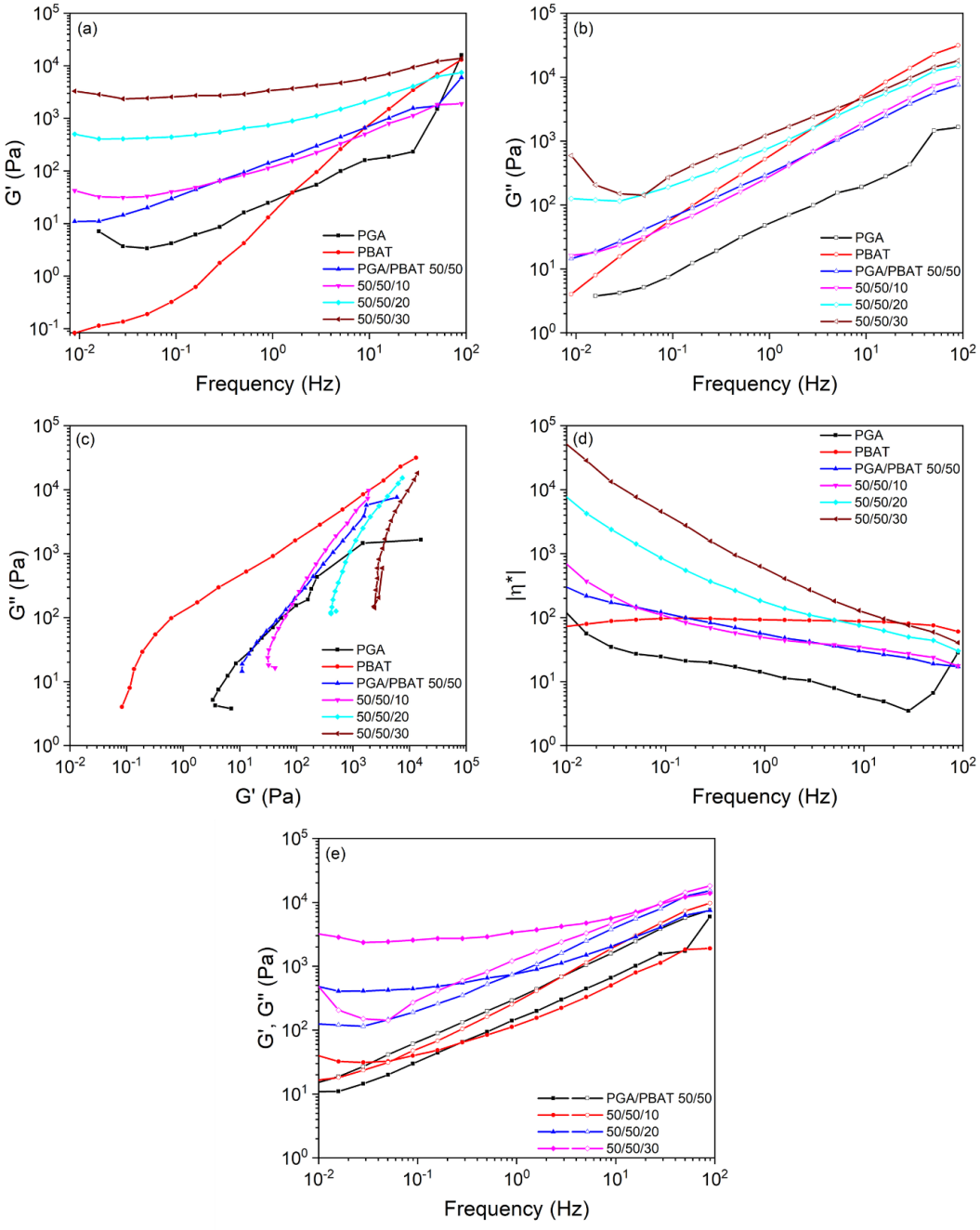

Figure 3: Rheological behaviour of PGA, PBAT and PGA/PBAT (50/50) blends on addition of EMA-GMA at loadings up to 30 wt. % at 240 °C: (a) storage modulus (G′), (b) loss modulus (G″), (c) Cole-Cole plot, (d) complex viscosity (|η*|) and (e) G′, G″, where filled symbols represent storage modulus, open ones represent loss modulus.

Film packaging applications require materials which possess a high tensile strength (>8 MPa), high strain at break (~150%) and an elastic modulus of ~100 – 200 MPa. Tensile testing results showed the effect of PGA/PBAT compatibilization through EMA-GMA addition. While the average tensile stress and elastic modulus of pristine PGA was 123.7 ± 21.4 MPa and 7600 ± 1200 MPa respectively and, for pristine PBAT was 24.1 ± 1.9 MPa and 101 ± 30 MPa respectively, the uncompatibilized 50/50 blend had an average tensile stress of 7.5 ± 0.6 MPa and elastic modulus of 407 ± 80 MPa. PGA had an average strain at break of 5 ± 3.8% whilst PBAT was 774 ± 61.3%. The uncompatibilized 50/50 blend exhibited an average strain at break of 10.7 ± 8.3%, suggesting that the PGA and PBAT phases are not compatible, as seen from the SEM imaging and FTIR analysis of this blend. However, the tensile strength and the elongation at break of the PGA/PBAT blends improved with the addition of EMA-GMA. There was a marginal increase in the tensile stress and elastic modulus from 7.5 ± 0.6 MPa to 10 ± 0.4 MPa for 50/50/10 and to 10.5 ± 0.5 MPa for 50/50/20 blends, respectively. Although, there was a significant enhancement in the elongation at break with addition of 10 wt. % and 20 wt. % EMA-GMA, there was no improvement in the elongation at break after 20 wt. % which suggests that EMA-GMA is an effective compatibilizer for the PGA/PBAT (50/50) blend only at concentrations <30 wt. %. Furthermore, the elastic modulus for 10, 20 and 30 wt. % addition of EMA-GMA indicated that the polymer blends were within the ideal 100 – 200 MPa range, at 102 ± 30, 150 ± 20 and 146 ± 50 MPa respectively. PGA/PBAT/EMA-GMA (50/50/20) showed the highest elongation at break of 145.2 ± 16.8% and tensile stress compared to PGA/PBAT (50/50), with the stress-strain curves of the blends shown in Figure 4, and the stress-strain curves of PGA and PBAT shown in Figure S1. The bump in the stress-strain curves for 50/50/20 and 50/50/30 at ~110 – 120% was due to the increase in crosshead speed of the tensile tester as the sample testing speed was increased from 10 mm/min to 25 mm/min for observing the strain at break.

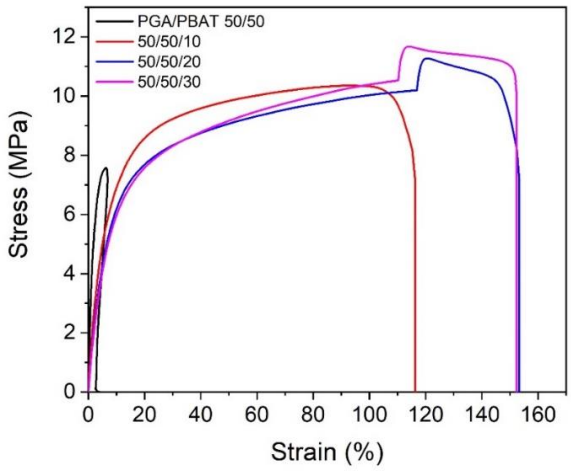

Figure 4: Stress-strain curves of PGA/PBAT 50/50 with 10, 20 and 30 wt. % inclusion of EMA-GMA. (The kink at strain around 110 % is due to the change in strain rate from 10 mm/ min to 25 mm/min until the sample broke)

Figure 5 compares the mechanical properties of PGA/PBAT/EMA-GMA (50/50/20) blends obtained with other biodegradable blends reported previously. Evidently, the PGA/PBAT (50/50) blend exhibits low extension at break (<120%), similar to pristine polymers like PGA, PLA and PLGA. With inclusion of EMA-GMA as a compatibilizer, the blends exhibited extension at break ~150% which is a key requirement for flexible packaging films.

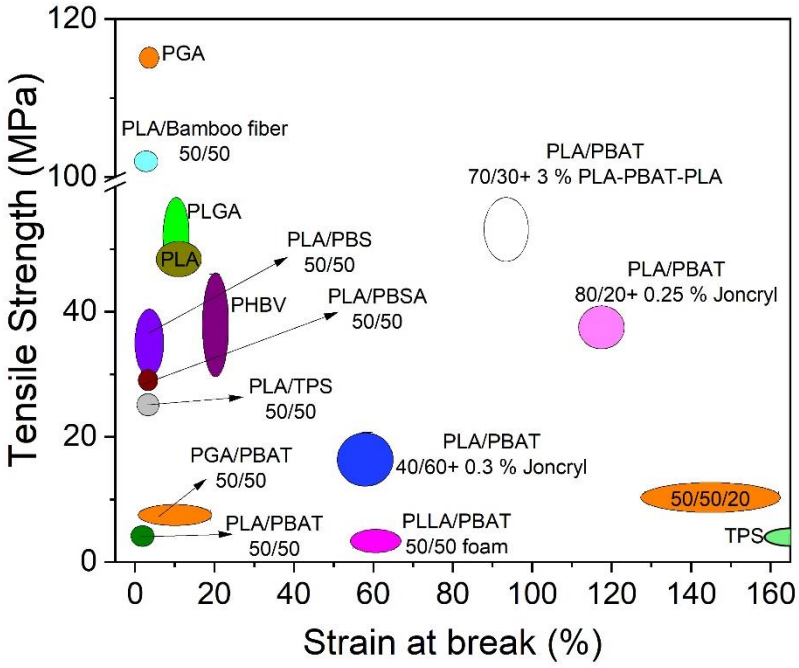

Figure 5: Mechanical properties of biodegradable co-continuous polymer blends from the literature. 70/30 and 80/20 blends of PLA/PBAT, pristine polymers are shown for comparison. The values plotted are taken from references [4, 24-33] Orange colour represents the results from this work.

The effect of compatibilization on the permeability of the polymer blends to oxygen and water vapour was investigated, a key consideration for use in biodegradable food packaging applications. Figure 6 a) and b) shows the permeability data for oxygen ($P'O_2$ at 23 °C, 0% RH and 50% RH) and water vapor (P′WV at 23 °C and 65% RH) for the polymer blends used in this study, respectively. The PGA used in this study could not be processed by itself with sufficient quality, therefore literature values for PGA by Kureha have an oxygen permeability of 0.013 (cm^3 mm) / (m^2 24h atm) at 20 °C and 80% RH[34] while from our study we observed the oxygen permeability of PBAT as 82.1 (cm^3 mm) / (m^2 24h atm) at 23°C and 50% RH. As PGA and PBAT are incompatible, the average oxygen permeability of PGA/PBAT 50/50 was 124.73 (cm^3 mm) / (m^2 24h atm). The addition of 10 wt. % EMA-GMA resulted in a large increase in the oxygen permeability, partly due to the presence of phase separation still in this sample (Figure 1 b)). The increase of EMA-GMA to 20 wt. % and 30 wt. % led to a decrease in the oxygen permeability to 102.6 (cm^3 mm) / (m^2 24h atm) compared to the compatibilized polymer blend. This is partly attributed to compatibilization of PGA and PBAT (Figure 1 c), d)).

The water vapour permeability of PGA was reported to be WP = 0.165 (g mm) / (m^2 24h atm) at 40 °C and 90% RH[34] while from our experiments, PBAT showed an average water vapour permeability of 6.34 (g mm) / (m^2 24h atm) at 23°C and 65% RH. A decrease of ~ 40% in the average water vapour permeability was obtained for the PGA/PBAT 50/50 blend. An additional improvement in the water vapour barrier performance was observed upon the addition of 10 wt. % and 20 wt. % EMA-GMA (~ 40% and ~ 47%, respectively, over the PGA/PBAT 50/50 sample), whilst no further improvements in water vapour barrier performance were observed for 30 wt. % EMA-GMA.

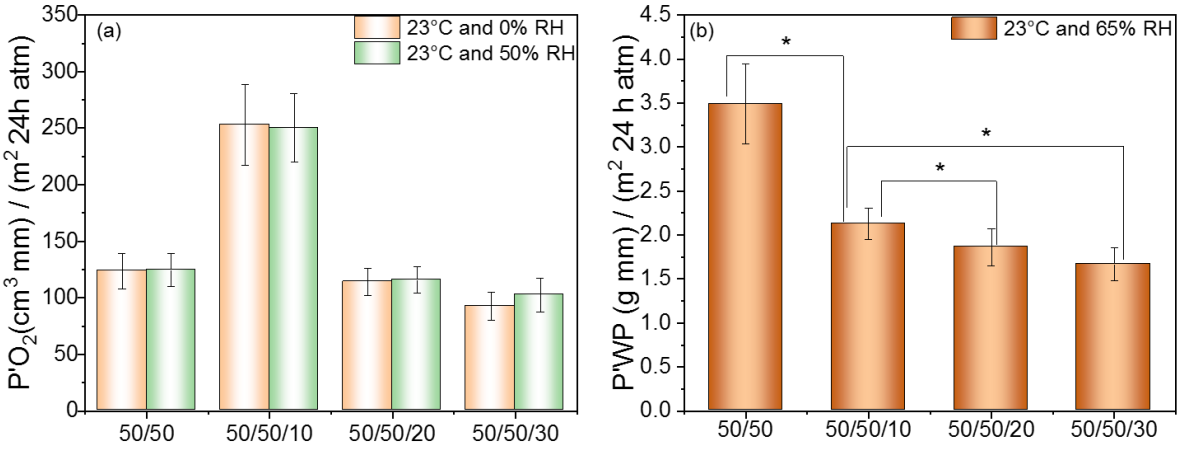

Figure 6: (a) Oxygen and (b) water vapour permeability data for PGA/PBAT/EMA-GMA blends. (* in the figures indicate a statistical significant difference which was determined ANOVA post-hoc analysis with $p<0.05$ and n=3 specimen per sample.)

Table 1 Thermal transitions for PGA, PBAT and PGA/PBAT based blends from first cooling cycle and second heating cycle.

Sample	T_g (°C) PBAT	T_g (°C) PGA	T_m (°C) PGA	T_c (°C) PGA	T_m (°C) PBAT	T_c (°C) PBAT	% X_c PGA	%X_c PBAT
PGA	-	51.4	214.2, 221.3	192.7	-	-	44.7	-
PBAT	-28.7	-	-	-	118.6	75.9	-	9.4
PGA/PBAT 50/50	-28.9	-	206.8, 216.2	190.5	120.1	83.9	37.2	10.5
50/50/10	-28.0	37.9	207.4, 217.5	190.5	120.8	83.9	45.1	3.6
50/50/20	-30.2	38.5	211.6, 220.5	194.0	120.0	77.1	46.9	7.1
50/50/30	-29.7	39.4	211.1, 220.3	192.5	119.9	77.4	37.4	10.5

To understand how the physical properties of the polymer blend affect the gas barrier properties, differential scanning calorimetry (DSC) was used to investigate how the crystallinity of PGA and PBAT are affected, shown in Table 1 and the first cooling and second heating curves shown in Figure S2. Crystallinity in PGA forms due to the interaction between C-H and O=C-H bonds along the polymer chain, producing hedrite crystal structures which vary in size depending on thermal expansion from heating.[35] For PBAT, the crystallinity formed specifically depends on the ratio between butylene adipate (BA) and butylene terephthalate (BT): a BT ratio of less than 20 mol% means that BT crystallizes in a BA lattice; a BT ratio of greater than 30 mol% means that BT crystallizes in a BT lattice; a BT ratio of 20 – 30 mol% means that BT crystallizes in a mix of BA and BT lattice.[36-38] Upon addition of 10% EMA-GMA, a large decrease in the crystallinity of PBAT is observed with respect to PGA/PBAT 50/50, corresponding to a large increase in oxygen permeability, likely due to EMA-GMA preferentially interacting with PBAT and disrupting the crystal structures formed. In addition, a double melt peak is observed in PGA, with the lower temperature melt peak ascribed to primary crystals melting and the higher temperature peak ascribed to melting of recrystallized crystals formed during heating by melt recrystallization. As the PBAT crystallinity increases again upon compatibilization between PGA and PBAT for 20 and 30% EMA-GMA, the oxygen permeability decreases again. The PGA crystallinity decreases for 50/50/30 due to the compatibilization of PGA and PBAT disrupting PGA crystal formation.

However, the water vapour permeability decreases across all samples upon addition of EMA-GMA, despite the overall crystallinity of the blends decreasing between 20 and 30 wt. % EMA-GMA. This suggests that the increase in the hydrophobic EMA-GMA content also reduced the water vapour permeability.

Table 2 compares the oxygen and water vapour permeability obtained in this work, compared to current commercially available polymer films. Some petrochemical derived polymers exhibit lower oxygen and water vapour permeability, but non-degradable plastic waste disposal issues and efforts to move towards use of sustainable and biodegradable polymers hinders their future for packaging applications. Comparatively, both PGA and PBAT individually are 100% biodegradable, and whilst biodegradability of the polymer blends in this is part of the future steps for this work, their barrier properties are comparable to conventional polymers, demonstrating their suitability for packaging applications.

Table 2: Comparison of oxygen and water vapour permeability of commercial polymer films[39] with the present work.

Polymers	$P'O_2$ (cm^3 mm) / (m^2 24h atm)	P′WV (g mm) / (m^2 24h atm)
BASF Terluran ABS film	45.6 – 81	3.1
Dow Acrylonitrile ABS films	47 – 102	2.0 - 6.3
Dow Trycite Oriented PS film	98 – 138	1.3
BASF AG Polystyrol 168 N GPPS Film	101	1.2
High Density Polyethylene (HDPE)	26.3 - 98.5	0.1 - 0.24
Mid Density Polyethylene (MDPE)	98.5 – 210	0.4 - 0.6
Low Density Polyethylene (LDPE)	98 – 453	0.39 - 0.59
DuPont Mylar films polyethylene naphthalate (PEN)	1.13 - 1.18	0.38 - 0.57
Fluorinated ethylene propylene (FEP)	295 – 394	0.087
Polytetrafluoroethylene (PTFE)	222 – 387	0.0045 - 0.30
Ethylene vinyl alcohol (EVOH)	0.01 - 0.15	0.8 - 2.4
Polyvinylidene chloride (PVDC)	0.00425 - 0.57	0.025 - 0.913
DOW Saran PVDC films	0.00425 - 0.00625	
PBAT (this work)	71.4 - 92.8*	5.58 - 7.1**
PGA/PBAT 50/50 (this work)	110.03 - 139.43*	3.04 - 3.94**
PGA/PBAT/AX8900 50/50/20 (this work)	104.01 - 128.01*	1.65 – 2.07**

* At 23°C and 50% RH, ** At 23°C and 65% RH

CONCLUSIONS

Overall, this work demonstrates the use of EMA-GMA to compatibilize PGA and PBAT for potential use in film packaging applications. The addition of 20 wt. % EMA-GMA is required to achieve useful compatibilization, and prevent phase separation due to only partial PGA miscibility with EMA-GMA. The mechanism for compatibilization, shown from FTIR measurements, is due to grafting of EMA-

GMA to PBAT hydroxyl chain ends and PGA hydrogen bonding with the resulting hydroxyl group formation from the grafting reaction. Once full compatibilization was achieved, PGA/PBAT/EMA-GMA 50/50/20 showed high tensile strength (10.5 MPa) and strain at break (145.2%), suitable for film packaging applications. Furthermore, the gas barrier properties for both oxygen permeability and water vapour permeability were shown to decrease upon the addition of 20 and 30 wt. % EMA-GMA, whereby an oxygen permeability of 102.6 (cm^3 mm) / (m^2 24h atm) and a water vapour permeability of 1.65 (g mm) / (m^2 24h atm) was observed. This was attributed to the increase in crystallinity of the polymer blends from increased compatibilization, whilst the water vapour permeability also decreased due to the EMA-GMA hydrophobicity.

REFERENCES

(1) Razza, F.; Innocenti, F. D. Bioplastics from renewable resources: the benefits of biodegradability. *Asia-Pac. J. Chem. Eng.* **2012,** *7*, S301-S309.
(2) Lackner, M. Bioplastics. *Kirk-Othmer Encyclopedia of Chemical Technology* **2000**, 1-41.
(3) *Bioplastics Market Development Update*; European Bioplastics: Berlin, Germany, 2020.
(4) Samantaray, P. K.; Little, A.; Haddleton, D. M.; McNally, T.; Tan, B.; Sun, Z.; Huang, W.; Ji, Y.; Wan, C. Poly(glycolic acid) (PGA): a versatile building block expanding high performance and sustainable bioplastic applications. *Green Chem.* **2020,** *22* (13), 4055-4081.
(5) Jem, K. J.; Tan, B. The development and challenges of poly (lactic acid) and poly (glycolic acid). *Adv. Ind. Eng. Polym. Res.* **2020,** *3* (2), 60-70.
(6) Moustafa, H.; El Kissi, N.; Abou-Kandil, A. I.; Abdel-Aziz, M. S.; Dufresne, A. PLA/PBAT Bionanocomposites with Antimicrobial Natural Rosin for Green Packaging. *ACS Appl. Mater. Interfaces* **2017,** *9* (23), 20132-20141.
(7) Witt, U.; Einig, T.; Yamamoto, M.; Kleeberg, I.; Deckwer, W. D.; Muller, R. J. Biodegradation of aliphatic-aromatic copolyesters: evaluation of the final biodegradability and ecotoxicological impact of degradation intermediates. *Chemosphere* **2001,** *44* (2), 289-99.
(8) Jiang, L.; Wolcott, M. P.; Zhang, J. Study of biodegradable polylactide/poly (butylene adipate-co-terephthalate) blends. *Biomacromolecules* **2006,** *7* (1), 199-207.
(9) Dong, W.; Zou, B.; Yan, Y.; Ma, P.; Chen, M. Effect of Chain-Extenders on the Properties and Hydrolytic Degradation Behavior of the Poly (lactide)/Poly (butylene adipate-co-terephthalate) Blends. *Int. J Mol. Sci.* **2013,** *14* (10), 20189-20203.
(10) Correa-Pacheco, Z. N.; Black-Solís, J. D.; Ortega-Gudiño, P.; Sabino-Gutiérrez, M. A.; Benítez-Jiménez, J. J.; Barajas-Cervantes, A.; Bautista-Baños, S.; Hurtado-Colmenares, L. B. Preparation and characterization of bio-based PLA/PBAT and cinnamon essential oil polymer fibers and life-cycle assessment from hydrolytic degradation. *Polymers* **2020,** *12* (1), 38.
(11) Han, Y.; Shi, J.; Mao, L.; Wang, Z.; Zhang, L. Improvement of Compatibility and Mechanical Performances of PLA/PBAT Composites with Epoxidized Soybean Oil as Compatibilizer. *Ind. Eng. Chem. Res.* **2020,** *59* (50), 21779-21790.
(12) Ma, P.; Cai, X.; Zhang, Y.; Wang, S.; Dong, W.; Chen, M.; Lemstra, P. J. In-situ compatibilization of poly(lactic acid) and poly(butylene adipate-co-terephthalate) blends by using dicumyl peroxide as a free-radical initiator. *Polym. Degrad. Stab.* **2014,** *102*, 145-151.
(13) Dong, W.; Zou, B.; Ma, P.; Liu, W.; Zhou, X.; Shi, D.; Ni, Z.; Chen, M. Influence of phthalic anhydride and bioxazoline on the mechanical and morphological properties of biodegradable poly(lactic acid)/poly[(butylene adipate)-co-terephthalate] blends. *Polym. Int.* **2013,** *62* (12), 1783-1790.
(14) Lin, S.; Guo, W.; Chen, C.; Ma, J.; Wang, B. Mechanical properties and morphology of biodegradable poly(lactic acid)/poly(butylene adipate-co-terephthalate) blends compatibilized by transesterification. *Mater. Des.* **2012,** *36*, 604-608.

(15) Sarul, D. S.; Arslan, D.; Vatansever, E.; Kahraman, Y.; Durmus, A.; Salehiyan, R.; Nofar, M. Preparation and characterization of PLA/PBAT/CNC blend nanocomposites. *Colloid Polym. Sci.* **2021**, 1-12.
(16) da Silva, J. M. F.; Soares, B. G. Epoxidized cardanol-based prepolymer as promising biobased compatibilizing agent for PLA/PBAT blends. *Polym. Test.* **2021,** *93*, 106889.
(17) Abdelwahab, M. A.; Jacob, S.; Misra, M.; Mohanty, A. K. Super-tough sustainable biobased composites from polylactide bioplastic and lignin for bio-elastomer application. *Polymer* **2021,** *212*, 123153.
(18) de Matos Costa, A. R.; Crocitti, A.; Hecker de Carvalho, L.; Carroccio, S. C.; Cerruti, P.; Santagata, G. Properties of Biodegradable Films Based on Poly(butylene Succinate) (PBS) and Poly(butylene Adipate-co-Terephthalate) (PBAT) Blends. *Polymers* **2020,** *12* (10), 2317.
(19) Sato, H.; Miyada, M.; Yamamoto, S.; Raghunatha Reddy, K.; Ozaki, Y. C–H···O (ether) hydrogen bonding along the (110) direction in polyglycolic acid studied by infrared spectroscopy, wide-angle X-ray diffraction, quantum chemical calculations and natural bond orbital calculations. *RSC Adv.* **2016,** *6* (20), 16817-16823.
(20) Yao, S.-F.; Chen, X.-T.; Ye, H.-M. Investigation of Structure and Crystallization Behavior of Poly(butylene succinate) by Fourier Transform Infrared Spectroscopy. *J. Phys. Chem. B* **2017,** *121* (40), 9476-9485.
(21) Rosa, B. d. S.; Merlini, C.; Livi, S.; Barra, G. M. d. O. Development of Poly (butylene adipate-co-terephthalate) Filled with Montmorillonite-Polypyrrole for Pressure Sensor Applications. *Mater. Res.* **2019,** *22* (2), e20180541.
(22) Shechter, L.; Wynstra, J. Glycidyl ether reactions with alcohols, phenols, carboxylic acids, and acid anhydrides. *Ind. Eng. Chem.* **1956,** *48* (1), 86-93.
(23) Zhang, K.; Nagarajan, V.; Misra, M.; Mohanty, A. K. Supertoughened Renewable PLA Reactive Multiphase Blends System: Phase Morphology and Performance. *ACS Appl. Mater. Interfaces* **2014,** *6* (15), 12436-12448.
(24) Homklin, R.; Hongsriphan, N. Mechanical and thermal properties of PLA/PBS co-continuous blends adding nucleating agent. *Energy Procedia* **2013,** *34*, 871-879.
(25) Kang, Y.; Chen, P.; Shi, X.; Zhang, G.; Wang, C. Preparation of open-porous stereocomplex PLA/PBAT scaffolds and correlation between their morphology, mechanical behavior, and cell compatibility. *RSC Adv.* **2018,** *8* (23), 12933-12943.
(26) Barbosa, J. D. V.; Azevedo, J. B.; Araújo, E. M.; Machado, B. A. S.; Hodel, K. V. S.; Mélo, T. J. A. d. Bionanocomposites of PLA/PBAT/organophilic clay: preparation and characterization. *Polímeros* **2019,** *29* (3), e2019045.
(27) Nofar, M.; Salehiyan, R.; Ciftci, U.; Jalali, A.; Durmuş, A. Ductility improvements of PLA-based binary and ternary blends with controlled morphology using PBAT, PBSA, and nanoclay. *Composites, Part B* **2020,** *182*, 107661.
(28) Arruda, L. C.; Magaton, M.; Bretas, R. E. S.; Ueki, M. M. Influence of chain extender on mechanical, thermal and morphological properties of blown films of PLA/PBAT blends. *Polym. Test.* **2015,** *43*, 27-37.
(29) Ding, Y.; Lu, B.; Wang, P.; Wang, G.; Ji, J. PLA-PBAT-PLA tri-block copolymers: Effective compatibilizers for promotion of the mechanical and rheological properties of PLA/PBAT blends. *Polym. Degrad. Stab.* **2018,** *147*, 41-48.
(30) Al-Itry, R.; Lamnawar, K.; Maazouz, A. Improvement of thermal stability, rheological and mechanical properties of PLA, PBAT and their blends by reactive extrusion with functionalized epoxy. *Polym. Degrad. Stab.* **2012,** *97* (10), 1898-1914.
(31) Okubo, K.; Fujii, T.; Yamashita, N. Improvement of interfacial adhesion in bamboo polymer composite enhanced with micro-fibrillated cellulose. *JSME Int. J., Ser. A* **2005,** *48* (4), 199-204.
(32) Mittal, V.; Akhtar, T.; Matsko, N. Mechanical, thermal, rheological and morphological properties of binary and ternary blends of PLA, TPS and PCL. *Macromol. Mater. Eng.* **2015,** *300* (4), 423-435.
(33) Li, G.; Favis, B. D. Morphology Development and Interfacial Interactions in Polycaprolactone/Thermoplastic-Starch Blends. *Macromol. Chem. Phys.* **2010,** *211* (3), 321-333.
(34) Murcia Valderrama, M. A.; van Putten, R. J.; Gruter, G. M. PLGA Barrier Materials from CO2. The influence of Lactide Co-monomer on Glycolic Acid Polyesters. *ACS Appl. Polym. Mater.* **2020,** *2* (7), 2706-2718.

(35) Yu, C.; Bao, J.; Xie, Q.; Shan, G.; Bao, Y.; Pan, P. Crystallization behavior and crystalline structural changes of poly(glycolic acid) investigated via temperature-variable WAXD and FTIR analysis. *CrystEngComm* **2016,** *18* (40), 7894-7902.
(36) Jian, J.; Xiangbin, Z.; Xianbo, H. An overview on synthesis, properties and applications of poly(butylene-adipate-co-terephthalate)–PBAT. *Adv. Ind. Eng. Polym. Res.* **2020,** *3* (1), 19-26.
(37) Gan, Z.; Kuwabara, K.; Yamamoto, M.; Abe, H.; Doi, Y. Solid-state structures and thermal properties of aliphatic–aromatic poly(butylene adipate-co-butylene terephthalate) copolyesters. *Polym. Degrad. Stab.* **2004,** *83* (2), 289-300.
(38) Cranston, E.; Kawada, J.; Raymond, S.; Morin, F. G.; Marchessault, R. H. Cocrystallization Model for Synthetic Biodegradable Poly(butylene adipate-co-butylene terephthalate). *Biomacromolecules* **2003,** *4* (4), 995-999.
(39) Abbott, S. Permeability Calculations. https://www.stevenabbott.co.uk/practical-coatings/permeability.php (accessed 28 January).